Lasers in Surgery and Medicine 21:149–158 (1997)

Ultraviolet Laser-induced Fluorescence of Human Stomach Tissues: Detection of Cancer Tissues by Imaging Techniques

Barbara W. Chwirot,* Dr Hab, Stanisław Chwirot, Dr Hab, Waldemar Jędrzejczyk, Prof Dr Hab, Marek Jackowski, PhD, Anna M. Raczyńska, PhD, Jacek Winczakiewicz, MD, and Joanna Dobber

Interdisciplinary Group of Optical Methods of Early Detection of Cancer, Nicholas Copernicus University, PL 87-100 Toruń, Poland

Background and Objective: **The background for this work was several literature reports on applications of the fluorescence methods to detection and localization of human cancers. The objective of our study has been to investigate if such an approach could be applied for the detection of gastric cancers.**
Study Design/Materials and Methods: **Our study was designed in such a way that spectrally resolved images of laser-induced fluorescence of human gastric mucosa were collected and assessed from a point of view of elaborating an algorithm allowing for a differentiation between malignant and premalignant lesions and areas of normal mucosa. The method involved exciting the autofluorescence with ultraviolet light (325 nm, He-Cd laser). The images were recorded in vitro in six regions of a visible spectrum using a cooled CCD camera. The material for study was 21 resected specimens for which altogether 72 surface areas were examined.**
Results: **The main result is the observation that a difference of the fluorescence intensities measured at 440 nm and 395 nm, both normalized to intensity measured at 590 nm, differs significantly for the tissues of interest.**
Conclusion: **Using that difference as a diagnostic parameter, it was possible to classify malignant tumor tissues with a sensitivity of 96% and a predictive value of 42%, whereas the same approach applied to abnormal but not tumor stomach tissues gave values of 80% and 98%, respectively. Lasers Surg. Med. 21: 149–158, 1997.** **© 1997 Wiley-Liss, Inc.**

Key words: autofluorescence imaging; cancer diagnostics; early diagnosis; fluorescence; gastric malignancies; native fluorescence; noninvasive; optical biopsy; optical spectroscopy

INTRODUCTION

Gastrointestinal malignancies are a major problem worldwide. The estimated incidence rate of gastrointestinal cancers is second only to lung cancer, although the scale of the problem differs significantly between different countries. In Poland as in Japan, gastric cancer is still recognized as a leading health problem [e.g., see 1,2].

Modern methods of detecting cancers of the stomach rely generally on endoscopy and histological analyses of gastrobiopsies and less often on additional radiological and/or ultrasonographic examinations. Gastric carcinomas show little response to chemotherapy, and therefore early detection of malignant or premalignant lesions is of a crucial importance for a success in surgical

Contract grant sponsor: Komitet Badań Naukowych; Contract grant number: S4/93/05; Contract grant sponsor: Regional Fund of Environment Protection, Toruń, Poland.

*Correspondence to: Dr. Barbara W. Chwirot, Institute of Biology and Environment Protection, Nicholas Copernicus University, ul. Gagarina 9, PL 87-100 Toruń, Poland.

Accepted 25 September 1996.

treatment. In spite of progress in the field of the diagnostics, the majority of patients still start treatment at a late stage of the disease. Well-established screening programs based on a very wide application of endoscopy resulted in 27–33% detection of early stages of gastric cancers in Japan; in Poland the same parameter reaches only 5–8%.

A new approach to the problem of medical diagnostics, especially of malignant and premalignant lesions, is the use of methods of optical spectroscopy [3]. The rationale behind this method is that the observation of the optical characteristics of tissues such as absorption or fluorescence may yield information on tissue composition, architecture, and physiological state. Endogenous fluorescent components of the cells are either their structural elements or molecules involved in metabolic processes. Thus there is no doubt that changes both in the structure of the tissue and/or cells, as well as in their metabolism, affect photophysical properties of the system. The problem is, however, if the changes reflecting occurrence of pathologies can be detected and identified on a background of natural variations due to a scatter of optical properties of tissues of different individuals as well as to age, biological cycles, history of individual health problems, previous pharmacological treatments, and several other internal or external factors.

First reports on studies on a possibility of diagnostic application of natural fluorescence of human tissues were published in 1987 [4,5]. Tissues accessible via endoscopy were a natural target of such research, and indeed, the first report was devoted to studies of laser-induced autofluorescence of several tissues including those of the stomach [4]. Those early results suggested that spectra from cancer regions located in different parts of a human body demonstrated characteristic peaks at 630 nm and 690 nm. Later studies did not confirm that optimistic conclusions of Yuanlong et al. [4] and Alfano et al. [5] suggested that the peaks reported by Yuanlong et al. [4] could be specific to buccal tissues, which formed a majority of tissues investigated by the Chinese group.

Generally, one can distinguish two different approaches to the problem of cancer diagnostics based on the following measurements of the autofluorescence.

1. The so-called optical biopsy methods involve exciting the fluorescence of tissues in a small area of a diameter on the order of 0.1–1.0 mm and recording a whole spectrum, which is then a source of the diagnostic information. Special mathematical procedures are used to find criteria allowing for a discrimination of the fluorescence spectra of neoplastic tissues from those of healthy ones [see, e.g., 7–9]. Similarly, in the case of a classical biopsy, it is the endoscopist who must decide what areas should be subject to examination. However, during the endoscopic procedure, the optical analysis of the autofluorescence may improve the accuracy of detection of cancerous lesions and help to decide on the location of biopsies. For that reason, the optical biopsy methods have been developed mostly for endoscopic examinations of colonic tissues with regard to distinguishing between hyperplastic and adenomatous polyps and discriminating between them and normal colonic mucosa.

2. The digital imaging method uses typically images of a whole field of view of the endoscope. The images are recorded using spectral filters and thus provide information on spatial distributions of the fluorescence intensities in different bands of the spectrum. The images are acquired and analyzed in real with with specially developed numerical procedures and if areas suspected of a malignant characteristic are detected, they are displayed on a monitor screen [e.g., 10]. The majority of the diagnostic algorithms involves rationing of the fluorescence emissions of different fluorophores, the approach first applied in this field by Alfano et al. [11]. In this way the endoscopist obtains objective information of the probable locations of cancerous lesions. Thus such methods can be considered more objective from those of the optical biopsy class.

At present, research in the field of optical detection of malignant and premalignant lesions concentrates mainly on colon and bronchial tissues. Other studies of modifications of the autofluorescence were concerned with neoplastic lesions in the skin [12], cervix [13, 14], and urinary bladder [15, 16]. The work on bronchial tissues resulted in a commercially available diagnostic unit (LIFE—lung imaging fluorescence endoscope) allowing for performing autofluorescence examinations of tissues in the area of the bronchial tree [17]. A pilot study on a possible use of a similar approach for the detection of laryngeal tumors was also reported in the literature [18].

In the present work, we report the first results of studies on a possibility of developing an autofluorescence imaging method for detecting gastric malignancies. The main goal was to perform in vitro feasibility studies using the digital imaging approach to detect cancerous lesions in

the stomach cavity and to develop a methodology for extending the research into in situ gastroscopic studies.

MATERIALS AND METHODS

The material for the study was specimens obtained from surgery of 21 patients with gastric carcinomas or other gastric problems qualifying them for surgical treatment. This study was approved by the District Committee of Ethics of Scientific Research at School of Medicine (Bydgoszcz, Poland).

Immediately after a resection, the tissue specimens were placed in containers with standard Ringers solution and transported to the laboratory. The spectroscopic measurements were typically carried out within 1–3 hours of tissue excision. During the measurements, the tissue specimens were kept on a cold table (+4°C) and wetted with the Ringers solution to avoid dehydration. At such conditions the samples did not show signs of hemolysis, which might result in staining the surfaces with hemoglobin. Some lesion were hemorrhagic, but such areas easily could be recognized. The intensity of the fluorescence signal was for them significantly lower than for all other tissues, and the effect has been already reported by several authors.

The whole procedure of taking images of the autofluorescence usually required up to 2 hours. Typically, seven images (white light illumination and six spectrally resolved images under a UV excitation) of the same area comprising a lesion and neighboring tissues were taken. Similar images of another area at a distance of several centimeters from the lesion and comprising tissues visually diagnosed as normal also were taken when possible. The specimens were then fixed in formalin and submitted for routine histopathological examination at the hospital pathology unit. The areas studied for their fluorescence were marked with pins to ensure a proper comparison of the results and histological evaluations.

Figure 1 presents a schematic diagram of the experimental set-up. A helium-cadmium laser (Omnichrome 2056-8/25M) operating at wavelengths of 325 and 442 nm was used to excite the tissue autofluorescence. The laser beam was first transmitted through a UV filter (3 layers of 1 mm thick UG11 filter) cutting off a visible 442 nm line and other nonlaser lines produced by a discharge in the laser tube and was then coupled via a lens into a single 200 μm quartz optical fiber (Ocean Optics). At the output aperture of the fiber, another lens system was used (Oriel 77646) to ensure defocusing of the beam and a homogeneous illumination of the area of interest. Typically, the intensity of the beam at a sample was on the order of ca. 0.5 mW/cm^2.

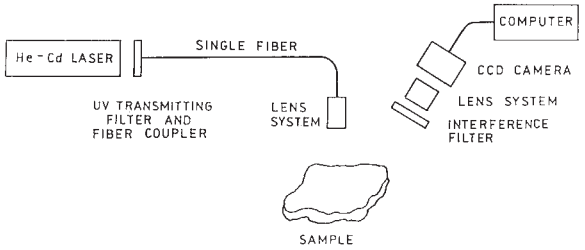

Fig. 1. Schematic diagram of the experimental set-up. Ultraviolet radiation from a helium-cadmium laser is delivered to the tissue specimen via optical fiber. Images of the autofluorescence of the tissues are taken using a CCD camera equipped with the interference filter transmitting light of suitable wavelengths.

The spectrally resolved images of the tissue fluorescence were taken using an imaging system based on a CCD camera (Lynxx 2, SpectraSource) designed for low light application and allowing for photometric measurements. The CCD element of the camera is cooled to −30°C and with a resulting low dark count rates allows for using long exposure times. The images were corrected for dark counts, bias voltages of the pixels, and also for variations in the sensitivity of the pixels of the CCD matric (flat field correction) according to procedures suggested by the manufacturer of the camera. The contrast, gray values, gain, etc., were always the same as required for photometric measurements. The optical system of the camera included a suitable interference filter and objective lens of a typical photographic camera (wide angle, f 37 mm) mounted at the camera using a set of distance rings. The interference filters were custom designed and were characterized by external transmittance of 50–65% and full widths at half maximum of 6–8 nm. The filters were centered at 380, 395, 440, 470, 560, and 595 nm. All filters cut off infrared radiation up to ~1 μm. Images of areas of ~10 cm^2 were taken from a distance of 30 cm to reduce errors of a determination of the intensity of the fluorescence due to different distances from different areas of the often folded surface of a sample. Exposure times were between 0.1–1,000 sec depending on the spectral range and to a less extent on the sample. Typically, images recorded at 395 nm and 595 nm required exposure times of ~700 sec, whereas the time of

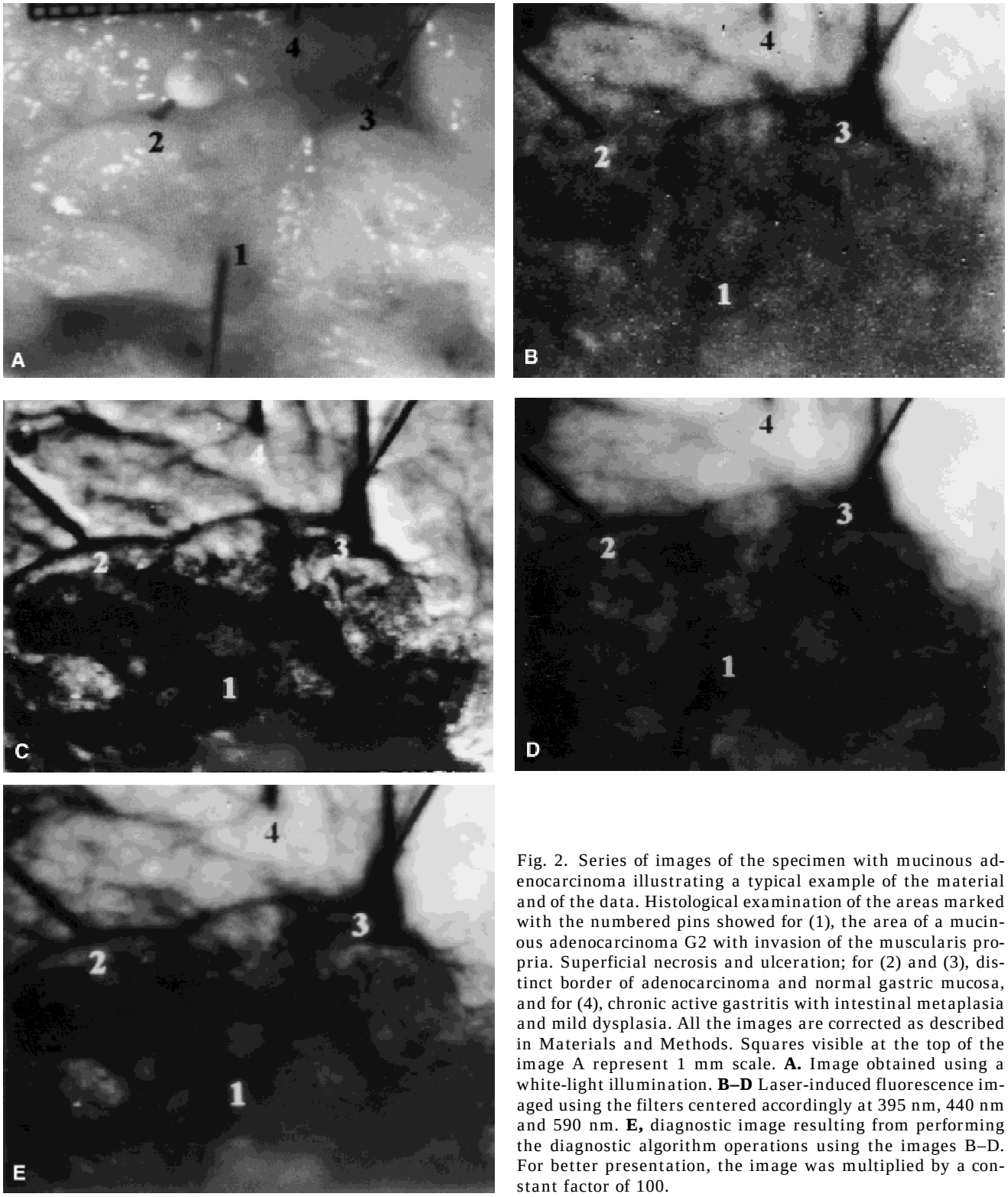

Fig. 2. Series of images of the specimen with mucinous adenocarcinoma illustrating a typical example of the material and of the data. Histological examination of the areas marked with the numbered pins showed for (1), the area of a mucinous adenocarcinoma G2 with invasion of the muscularis propria. Superficial necrosis and ulceration; for (2) and (3), distinct border of adenocarcinoma and normal gastric mucosa, and for (4), chronic active gastritis with intestinal metaplasia and mild dysplasia. All the images are corrected as described in Materials and Methods. Squares visible at the top of the image A represent 1 mm scale. **A.** Image obtained using a white-light illumination. **B–D** Laser-induced fluorescence imaged using the filters centered accordingly at 395 nm, 440 nm and 590 nm. **E,** diagnostic image resulting from performing the diagnostic algorithm operations using the images B–D. For better presentation, the image was multiplied by a constant factor of 100.

350 sec or less was sufficient at 440 nm and 470 nm. The signal-to-noise ratios varied with the exposure times and fluorescence intensities of the measured signals from ~0.01 (very low signal, very long exposure time) to ~100 (bright fluorescence and short exposure time). Typical images recorded in this work are shown in Figure 2a–d. As can be seen, typically the imaged areas of the

TABLE 1. Histological Description of Imaged Areas of Tissue Specimens*

No	Histological description of lesion	K	Type
1.	Inflammatory fibroid polyp, chronic active gastritis.	0.51	a
2.	Inflammatory fibroid polyp with superficial necrosis.	0.59	a
3.	As above.	0.48	a
4.	Anaplastic and signet-ring cell carcinoma with superficial necrosis.	0.59	c
5.	Diffuse infiltration of signet ring cell carcinoma. Superficial gastritis.	0.88	c
6.	Submucous diffuse infiltration of signet-ring cell carcinoma (praepyloric part).	1.22	a
7.	Normal structure of the fundic part.	1.01	n
8.	Adenocarcinoma G2 of the fundic part with superficial ulceration.	0.38	c
9.	Adenocarcinoma G2. Trabecular pattern. Superficial ulceration. Excessive lymphocytic infiltration.	0.52	c
10.	Active chronic gastritis with focal atrophy, intestinal metaplasia and mild dysplasia.	0.68	a
11.	As above.	0.40	a
12.	Active chronic gastritis with atrophy. Incomplete intestinal metaplasia. Lymphocytic infiltration.	0.74	a
13.	Chronic active erosive gastritis.	0.67	a
14.	Primary gastric intermediate grade lymphoma (centrocyte-like) of the pyloric part.	0.95	c
15.	Submucous diffuse infiltration of centrocyte-like lymphoma.	0.81	a
16.	Focal submucous infiltrations of centrocyte-like lymphoma.	0.85	a
17.	Gastric, fundic mucosa-normal structure.	1.18	n
18.	Adenocarcinoma G3. Trabecular pattern, partly signet-ring cell carcinoma with superficial ulceration. Desmoplastic and lymphocytic stromal reaction.	0.48	c
19.	Chronic antral gastritis (intestinal metaplasia and mild dysplasia).	1.25	a
20.	As above.	0.78	a
21.	Chronic antral gastritis with metaplasia and severe dysplasia. Excessive lymphocytic infiltration.	1.28	a
22.	Tubular adenocarcinoma G1. Superficial focal foeolar hyperplasia.	0.66	c
23.	Chronic active gastritis with focal intestinal metaplasia and dysplasia. Submucous invasion of adenocarcinoma.	0.68	a
24.	Chronic gastritis with intestinal focal metaplasia and mild dysplasia.	1.03	a
25.	Mucinous adenocarcinoma G2 with invasion of the muscularis propria. Superficial necrosis and ulceration.	0	c
26.	Distinct border of adenocarcinoma and normal gastric mucosa.	0.48	c
27.	Chronic active gastritis with focal intestinal metaplasia and mild dysplasia.	0.96	a
28.	Chronic active gastritis, foveolar hyperplasia, intestinal metaplasia and mild dysplasia.	0.65	a
29.	Chronic active gastritis with foveolar hyperplasia.	0.63	a
30.	Mucinous adenocarcinoma. Diffuse plasma cell infiltration.	0.65	c
31.	Chronic active gastritis with intestinal metaplasia and diffuse dysplasia.	1.11	a
32.	Chronic active gastritis with severe dysplasia.	1.01	a
33.	Chronic active gastritis with focal atrophy and severe dysplasia.	1.58	a
34.	Chronic erosive gastritis. Intestinal complete metaplasia and mild dysplasia.	0.58	a
35.	Chronic active gastritis with atrophy and mild dysplasia.	0.74	a
36.	Adenocarcinoma G3 diffuse infiltration. Superficial ulceration with lymphocytic and leucocytic reaction.	0.74	c
37.	Adenocarcinoma G3 partly solid, partly tubular pattern.	0.91	c
38.	Chronic active gastritis with atrophy. Intestinal metaplasia with mild dysplasia. Focal foveolar hyperplasia.	0.98	a
39.	Superficial gastric ulceration of the body with inflammatory reaction, intestinal metaplasia and mild dysplasia.	0.01	a
40.	Active chronic gastritis partly erosive.	0	a
41.	Chronic gastritis. Focal foveolar hyperplasia, focal intestinal metaplasia.	0.47	a
42.	Intramucous signet-ring cell carcinoma with superficial ulceration.	0.70	c
43.	Tubular adenocarcinoma G1 (deep submucous invasion).	0	c
44.	Signet-ring cell carcinoma with ulceration and inflammation. Focal tubular adenocarcinoma.	0.33	c
45.	Tubular adenocarcinoma of the pyloric mucosa. Stromal inflammatory reaction. Hyperplasia of the lymphoid tissue with prominent follicular differentiation.	0.33	c
46.	Antral gastritis with foveolar hyperplasia, intestinal incomplete metaplasia and lymphocytic infiltration.	0.59	a
47.	As above.	0.80	a
48.	Signet-ring cell carcinoma of superficial mucosa.	0	c
49.	Antral gastritis with foveolar hyperplasia, lymphoplasia, and intestinal incomplete metaplasia.	0.56	a
50.	Active chronic gastritis.	1.25	a

TABLE 1. Continued.

No	Histological description of lesion	K	Type
51.	Mild gastritis in the superficial part of fundic mucosa.	1.35	n
52.	Gastric, fundic mucosa-normal structure.	1.37	n
53.	Adenocarcinoma G3 (solid partly tubular pattern, deep invasion, desmoplasia).	0.53	c
54.	Chronic antral gastritis with intestinal metaplasia and dysplasia in the margin of cancer. Submucous invasion of solid cancer.	1.13	c
55.	Antral gastritis. Focal foveolar hyperplasia. Submucous invasion of cancer.	1.48	a
56.	Mild chronic gastritis (body mucosa).	1.34	a
57.	Mucinous adenocarcinoma (cardial region). Deep invasion. Lymphocytic infiltration.	0.09	c
58.	Submucous invasion. Foveolar hyperplasia with dysplasia.	0.44	a
59.	Mucosal structure normal. Submucous focal adenocarcinoma.	0.67	a
60.	Normal body mucosa.	0.94	n
61.	Adenocarcinoma G3 (solid partly tubular pattern).	0.68	c
62.	Gastritis. Submucous and intramural infiltration of adenocarcinoma.	0.88	a
63.	Chronic active gastritis with atrophy. Tubular adenocarcinoma of body mucosa. Diffuse submucous and intramural invasion.	0.94	c
64.	Chronic gastritis with foveolar hyperplasia and intestinal metaplasia.	0.98	a
65.	Primary gastric intermediate grade lymphoma (centrocyte-like).	0	c
66.	Distinct margin within the body mucosa.	0	c
67.	Mild chronic gastritis with lymphoplasia.	0	a
68.	As above.	0.38	a
69.	Mild chronic gastritis with lymphoplasia and foveolar hyperplasia.	0	a
70.	Mild antral gastritis.	0.99	a
71.	Active, chronic, antral gastritis with foveolar hyperplasia and intestinal incomplete metaplasia.	0.59	a
72.	Antral chronic gastritis with lymphoplasia and focal foveolar hyperplasia.	1.64	a

*Values of the Diagnostic Parameter Calculated by Performing With Images Mathematical Operations according to the formula for K and the classification (c — cancer, a — abnormal, n — normal) used for calculations of the diagnostic parameters of the method and for preparing the histogram presented in Figure 3.

specimen surface included regions of a different histological nature.

The maximum dose of the irradiation absorbed by the sample calculated for the exposure time of 1,000 sec, and the laser light intensity of 0.5 mW/cm^2 did not exceed 0.5 J/cm^2 and was probably much lower due to a reflection of the UV light at a wet sample surface. Using a UV light in vivo at such intensity level may provoke questions regarding a safety of the procedure. In our opinion the only risk factor can be a possible mutagenic action of the UV light used for the excitation of the fluorescence since we did not observe any clear indication of thermal effects. We also expect that the exposure times required for in vivo examinations will be significantly shorter due to better light collection efficiency of the input optics of endoscopic devices. The colonic tissues are normally never exposed to light, and they probably do not have protecting mechanisms typical for human skin cells. However, we believe that it is reasonable to assume that using the UV light used in this study should not cause a significant damage to human genetic system. The absorption spectra of DNA and proteins show a drop to a zero value at a wavelength of 325 nm [see, e.g., 19]. Moreover, the intensity of the UV component of the sun light measured at the earth's surface at a medium zenith angle is the range of 320–330 nm on the order of 0.3 mW/cm^2 [19], i.e., the total intensity of the UVB components of the sun light is much higher than applied in our experiment.

RESULTS

A total of 72 areas of 21 specimens were analyzed by imaging with autofluorescence. In Table 1 we present the list of all the sampled areas together with their short histological characteristics and the results of the proposed diagnostic approach. It should be noted that the material studied also included specimens of stomach ulcers that were investigated to test if it is possible to differentiate between gastric ulcer and malignant disease.

It has been generally observed for all the material in this study that the intensity of the autofluorescence of the tumor tissues was in all the spectral bands lower than that of the visually normal tissues from the same specimen. Such a conclusion agrees well with observations obtained by other authors for a series of several tumors studied at different excitation conditions [see, e.g., 8–10,15,16]. We do not present data on the mean

intensities measured at different spectral bands since we do not know the spectral characteristics of the camera and the recorded intensities could not be renormalized according to variations in a spectral sensitivity of the CCD element. Difficulties in obtaining complete specifications of the CCD elements have long been a source of a growing concern of the camera users [20].

Analyzing the results obtained for all specimens, we found that a low fluorescence intensity of particular areas cannot be considered a sufficient parameter to differentiate the fluorescence of malignant or premalignant tissues from that of normal ones. In the case of the stomach, only on very rare occasions can one find neoplastic lesions occurring in the neighborhood of normal healthy tissues. As a rule, histopathological pictures of the areas of interest are very complex and more often than not one finds simultaneously several abnormalities sometimes interlaced and/or overlapping with each other. Moreover, the intensities of the fluorescence of the malignant tissues may differ not only from one specimen to another, but also within one lesion. In the case of tubular adenocarcinoma, we find occasionally an enhancement of the fluorescence, whereas necrosis and haematomas result in a lower intensity. Similar observations also hold for anaplastic cancer and stomach ulcers. It should be noted as well that in the case of stomach ulcers, increased levels of the fluorescence were observed in areas of metaplasia and dysplasia.

It has been found that the intensity of the fluorescence in any of the spectral bands investigated was not a sufficient parameter to discriminate neoplasia from non-neoplastic tissues. In such a situation, it was necessary to look for another parameter allowing for the detection and localization of malignancies. It was obvious that the method should include a procedure compensating for the effects of folding and curvature of the surfaces under study. Such purely geometrical factors cause (especially during endoscopic examinations) changes in the intensity of a detected fluorescence light due to the distance and angle of both illumination and detection of light emitted by the excited fluorophores. A typical solution for the problem in diagnostic and remote sensing applications of imaging techniques is to use a principle of rationing, i.e., to normalize intensities detected in different spectral bands to the one showing the least variations in all areas of interest. The results obtained using the rationing of the images obtained at different spectral bands are also free of systematic errors due to long-term drifts in the sensitivity of the camera and its electronic system during the time required for the measurements of all the samples. The results of Kapadia et al. [7], Schomacker et al. [8], and Bottiroli et al. [9] regarding colonic tissues indicated that at different excitation conditions, the authors consistently observed very similar levels of the fluorescence of malignant and premalignant tissues and of normal mucosa in the spectral region close to 600 nm, and it has been decided to use the 590 nm data to normalize intensities measured in other regions of the spectrum. The best discrimination of the tumor tissues was obtained using as a diagnostic parameter a difference between normalized intensities measured with the filters centered at 440 nm and 395 nm. It has been found that the parameter

$$K = \frac{I_{440} - I_{395}}{I_{590}}$$

where I_λ is the intensity measured for a given pixel at a wavelength λ and reduced to a constant exposure time can be considered an indicator of the presence of tumor tissues in the area under study. After the analysis of all the cases subject to the fluorescence examination, we have found the best option is to take as the threshold value $K = 1.0$. As an example, we show in Figure 2e the spatial distribution of the K parameter (diagnostic image) obtained after performing the above defined operations on the images given in Figure 2b–d. The values of K presented in Table 1 together with histological description of the areas subject to investigation were calculated from such images as average value found for several pixels of the given diagnostic image close to the pin marking the region selected for histological examination. The malignant tissues are then characterized by values of $K < 1.0$. It should be pointed out here that the condition of $K < 1.0$ is not sufficient for a clear and definite determination of a neoplastic character of the tissues. Nevertheless, it makes it possible to identify two classes of tissues: (1) the tissues that are not necessarily normal but with a high probability do not show features of a malignant transformation ($K > 1.0$), and (2) the tissues demonstrating abnormalities (among them with a high probability the malignant ones). We should also stress that the threshold value of $K = 1$ is uniquely defined for our experimental set-up, and it will be different if one

uses for recording the spectrally resolved images, a camera of a different spectral sensitivity characteristic with different objective lenses and a different set of the filters. The threshold value probably will also have to be redefined in our future in vivo endoscopic studies, because of the influence of the optical transmission characteristics of the imaging fiber optics of the endoscope on the fluorescence intensities measured in different spectral bands.

The following parameters were used to determine the significance and accuracy of our diagnostic algorithm for analysis of the images of the spectrally resolved fluorescence with regard to the discrimination of malignant tumors and of the presence of tissue abnormalities (inflammation, dysplasia, metaplasia, neoplastic changes). (1) C_R—sensitivity toward neoplastic tissue. This parameter is calculated as a percentage of cases in which our method was successful in classifying the histologically detected malignant tissue as malignant. Only the cases of tissues histologically verified as malignant are taken into account to calculate C_R. (2) S_R—predictive value for neoplastic tissue. It is defined as a percentage of cases in which the tissues classified as abnormal were histologically confirmed as malignant. To find this parameter, one takes into account all the cases for which our method yielded $K < 1$ and calculates a fraction of that number corresponding to the tissues of that group found to be malignant in histological examinations. This parameter can be considered a probability that an area showing $K < 1$ is really of a malignant character. (3) U_R—false negative toward neoplastic tissue. This parameter is a percentage of cases for which our method failed to identify the malignant tissue as malignant. As such it gives a probability of missing malignant tissues while using the approach under consideration.

Similarly, to characterize our method with respect to detecting all the tissue abnormalities (both malignant and nonmalignant), one can calculate the quantities C_C, S_C and U_C. They are then defined as follows: (1) C_C is a sensitivity of the method toward tissue abnormalities. It is defined as a percentage of all the cases histologically shown to be different from normal for which the fluorescence method yielded $K < 1$. This parameter is a measure of a success of the proposed approach in detecting gastric tissue abnormalities of any kind. (2) S_C represents the predictive value for abnormal tissues. It is calculated as a percentage of cases in which the tissues classified as abnormal in the fluorescence examination were histologically confirmed as truly different from normal gastric tissues. In other words, S_C is the probability that an area showing $K < 1$ shows really characteristics of tissues abnormalities of some kind. (3) U_R—false negative toward abnormal tissues. This quantity is a percentage of cases in which our method gave $K > 1$ for the tissues found to be of abnormal character in the histological examination. It gives a probability of not recognizing the abnormal tissues during the fluorescence examination.

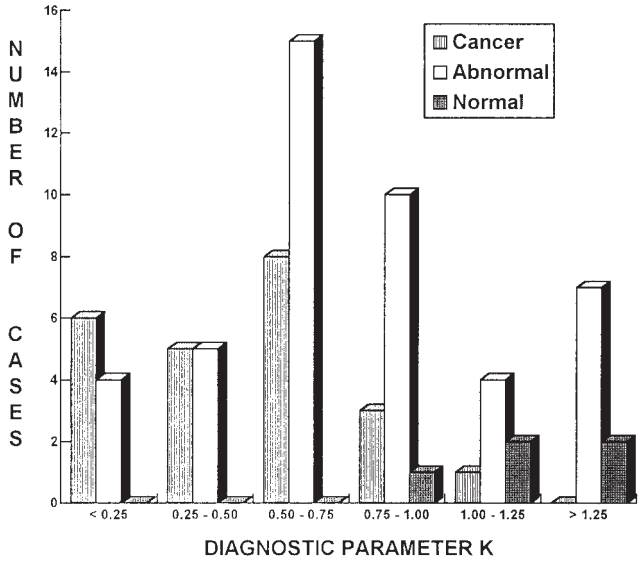

Fig. 3. Histogram for K parameter values calculated for tissues classified as malignant (cancer), showing abnormalities (abnormal) and normal. The K parameter is a difference of the intensities of the fluorescence imaged at the same exposure time using 440 nm and 395 nm filters and normalized to the intensity measured with the 590 nm filter.

A histogram for the K values calculated for all 72 histologically analyzed areas of images obtained for specimens representing our 21 patients is plotted in Figure 3. Assuming $K = 1.0$ as a threshold value for a discrimination of the malignant tissues, one determines a group of abnormal tissues with a sensitivity $C_C = 82\%$, and among those tissues the truly malignant ones with a sensitivity $C_R = 96\%$. It should be noted that despite a sensitivity of 96%, malignant tumors were detected in every specimen with gastric malignancy, and the sensitivity parameter is not 100%, because in one case one of three areas of adenocarcinoma yielded $K > 1$. The predictive value for neoplastic tissues seems relatively low, $S_R = 39\%$, but this does not seem to be a serious deficiency of the method since the predictive value for

tissue abnormalities is $S_C = 98\%$, and those areas should in any case be examined from the point of view of a further treatment. Such a conclusion is further supported by the fact that only in one case a histologically normal tissue was classified as abnormal, whereas the false negative value toward tumor tissues was $U_N = 4\%$ (one case of the malignant tissue classified as normal as described above) and the false negative value toward tissue abnormalities was $U_C = 18\%$. It can be seen from Table 1 that in eight cases of the submucous infiltration, the samples were classified as "abnormal" and not as "malignant." The reason for such a classification was that in those cases the malignant tissues probably did not contribute in a major way to the fluorescence signal. Nevertheless, it also can be seen that for those samples in six cases, the K value was significantly lower than one and thus only two such cases would be missed if one relied only on the results of the fluorescence examination.

DISCUSSION

In conclusion, our algorithm of analyzing the spectroscopically resolved images of the fluorescence of the tissues of a stomach wall allows for a discrimination of a group of the tissues that are suspected to be of a neoplastic character. The method when applied in vitro successfully detected practically all the specimens with gastric carcinomas (adenocarcinoma, anaplastic cancer, mucocellular cancer, and lymphoma) and additionally with a sensitivity of 80%, a wide group of tissue abnormalities such as fibroid polyp, intestinal metaplasia, dysplasia, ulcer, and inflammation.

The measurements in vitro necessarily yield data characteristic for tissues that are metabolically and biochemically different from similar tissues in vivo. Following Schomacker et al. [8], one can assume that the endogenous fluorophores responsible for the emission in 440 nm and 395 nm are, respectively, NADH and collagen. If this is indeed the case, one can expect that for the systems studied in vivo, it will be necessary to change the threshold value of the K parameter. As shown in Schomacker et al. [8], processes taking place in tissues after a resection may influence the fluorescence spectra. From the point of view of the present results, a very important observation of Schomacker et al. [8] was that the intensity of the NADH-related fluorescence decays exponentially after the resection with a time constant of 118 min. Although the system studied by Schomacker et al. [8] was colonic mucosa, it is reasonable to assume that similar processes take place in stomach tissues studied in vitro. Thus to evaluate a real diagnostic potential of the approach based on digital imaging of the spectrally resolved fluorescence, it is necessary to test it in endoscopic in vivo studies. Preparations for such tests are underway.

ACKNOWLEDGMENTS

This work was supported by grant Nr 0154/S4/93/05 (Komitet Badań Naukowych) and a grant from the Regional Fund of Environment Protection, Toruń, Poland.

REFERENCES

1. DeVita VT, Hellman S, Rosenberg SA, eds. "Cancer: Principles and Practice of Oncology." Philadelphia, Lippincott, 1993.
2. Zatoński W, Tyczyński J, eds. "Cancer in Poland in 1993". Warsaw, Department of Epidemiology and Cancer Prevention, National Cancer Registry, 1996.
3. Alfano RR, Tata DB, Cordeiro J, Tomashefsky P, Longo F, Alfano M. Laser induced fluorescence for native cancerous and normal tissue. IEEE-QE 1984; 20:1507–1511.
4. Yuanlong Y, Yanming Y, Fuming L, Yufen L, Paozhong M. Characteristic autofluorescence for cancer diagnosis and its origin. Lasers Surg Med 1987; 7:528–532.
5. Alfano RR, Tang GC, Pradhan A, Lam W, Choy DSJ, Opher E. Fluorescence spectra from cancerous and normal human breast and lung tissues. IEEE J Quantum Electron 1987; QE-23:1806–1811.
6. Alfano RR, Pradhan A, Tang GC, Das BB, Yoo KM. Optical spectroscopy may offer novel diagnostic approaches for the medical profession. In: Goldman L, ed. "Laser Non-Surgical Medicine: New Challenges for an Old Application." Lancaster-Basel, Technomic, 1991:55–124.
7. Kapadia CR, Cutruzzola FW, O'Brien KM, Stetz ML, Enriquez R, Deckelbaum LI. Laser-induced fluorescence spectroscopy of human colonic mucosa: Detection of adenomatous transformation. Gastroscopy 1990; 99:150–157.
8. Schomacker KT, Frisoli JK, Compton CC, Flotte TJ, Richter JM, Nishioka NS, Deutsch TF. Ultraviolet laser-induced fluorescence of colonic tissue: Basic Biology and Diagnostic Potential. Lasers Surg Med 1992; 12:63–78.
9. Bottiroli G, Croce AC, Locatelli D, Marchesini R, Pignoli E, Tomatis S, Cuzzoni C, Di Palma S, Dal Fante M, Spinelli P. Natural fluorescence of normal and neoplastic human colon: a comprehensive "ex vivo" study. Lasers Surg Med 1995; 16:48–60.
10. Hung J, Lam S, LeRiche JC, Palcic B. Autofluorescence of normal and malignant bronchial tissue. Lasers Surg Med 1991; 11:99–105.
11. Alfano RR, Das BB, Cleary J, Prudente R, Celmer E. Light sheds light on cancer. Bull NY Acad Med 1991; 67:143–150.
12. Lohman W. In situ differentiation between nevi and ma-

lignant melanomas by fluorescence measurements. Naturwissenschaften 1991; 78:456–457.
13. Sha Glassman W, Liu CH, Tang GC, Lubicz S, Alfano RR. Ultraviolet excited fluorescence spectra from non-malignant and malignant tissues of the gynecological tract. Lasers Life Sci 1992; 5:49–58.
14. Ramanujam N, Mitchell MF, Mahadevan A, Warren S, Thomsen E, Silva E, Richards-Kortum R. In vivo diagnosis of cervical intraepithelial neoplasia using 337 nm-excited laser-induced fluorescence. Proc Natl Acad Sci USA 1994; 91:10193–10197.
15. Cothren RM, Richards-Kortum R, Sivak Jr, MV, Fitzmaurice M, Rava RP, Boyce GA, Doxtrader M, Blackman R, Ivanc TB, Hayes GB, Feld MS, Petras RE. Gastrointestinal tissue diagnosis by laser-induced fluorescence spectroscopy at endoscopy. Gastrointest Endosc 1990; 36:105–111.
16. D'Hallewin MA, Baert L, Vanherzeele H. In vivo fluorescence detection of human bladder carcinoma without sensitizing agents. J Am Paraplegia Soc 1994; 17:161–164.
17. Lam S, MacAulay C, Palcic B. Detection and localization of early lung cancer by imaging techniques. Chest 1993; 103:12S–14S.
18. Harris ML, Lam S, MacAulay C, Qu J, Palcic B. Diagnostic imaging of the larynx: Autofluorescence of laryngeal tumours using the helium-cadmium laser. J Laryngol Otol 1995; 109:108–110.
19. Boeker E, van Grondelle R. "Environmental Physics." Chichester: Wiley & Sons, 1995.
20. Troy CT. A photonics spectra investigative report: How camera makers cope with a confused CCD market. Photonics Spectra 1996; 30:74–86.